THE JOURNAL OF BIOLOGICAL CHEMISTRY VOL. 285, NO. 16, pp. 12321–12333, April 16, 2010

Covalent Peroxisome Proliferator-activated Receptor γ Adduction by Nitro-fatty Acids

*SELECTIVE LIGAND ACTIVITY AND ANTI-DIABETIC SIGNALING ACTIONS**

Received for publication, December 3, 2009, and in revised form, January 15, 2010 Published, JBC Papers in Press, January 22, 2010, DOI 10.1074/jbc.M109.091512

Francisco J. Schopfer[‡1], Marsha P. Cole[‡1], Alison L. Groeger[‡1], Chen-Shan Chen[‡], Nicholas K. H. Khoo[‡], Steven R. Woodcock[‡], Franca Golin-Bisello[‡], U. Nkiru Motanya[‡], Yong Li[§], Jifeng Zhang[¶], Minerva T. Garcia-Barrio[‖], Tanja K. Rudolph[‡], Volker Rudolph[1**], Gustavo Bonacci[‡], Paul R. S. Baker[‡], H. Eric Xu[§], Carlos I. Batthyany[‡‡], Y. Eugene Chen[¶], Tina M. Hallis[§§], and Bruce A. Freeman[‡2]**

From the [‡]Department of Pharmacology and Chemical Biology, University of Pittsburgh, Pittsburgh, Pennsylvania 15261, the [**]Department of Cardiology, University Heart Center Hamburg, Hamburg 20246, Germany, the [‡‡]Institut Pasteur de Montevideo, Montevideo 11400, Uruguay, the [§]Laboratory of Structural Sciences, Van Andel Research Institute, Grand Rapids, Michigan 49503, the [¶]Department of Internal Medicine, Cardiovascular Center, University of Michigan Medical Center, Ann Arbor, Michigan 48109, [§§]Invitrogen Discovery Sciences, Madison, Wisconsin 53719, and the [‖]Cardiovascular Research Institute, Morehouse School of Medicine, Atlanta, Georgia 30310

The peroxisome proliferator-activated receptor-γ (PPARγ) binds diverse ligands to transcriptionally regulate metabolism and inflammation. Activators of PPARγ include lipids and anti-hyperglycemic drugs such as thiazolidinediones (TZDs). Recently, TZDs have raised concern after being linked with increased risk of peripheral edema, weight gain, and adverse cardiovascular events. Most reported endogenous PPARγ ligands are intermediates of lipid metabolism and oxidation that bind PPARγ with very low affinity. In contrast, nitro derivatives of unsaturated fatty acids (NO_2-FA) are endogenous products of nitric oxide ($^{\bullet}NO$) and nitrite (NO_2^-)-mediated redox reactions that activate PPARγ at nanomolar concentrations. We report that NO_2-FA act as partial agonists of PPARγ and covalently bind PPARγ at Cys-285 via Michael addition. NO_2-FA show selective PPARγ modulator characteristics by inducing coregulator protein interactions, PPARγ-dependent expression of key target genes, and lipid accumulation is distinctively different from responses induced by the TZD rosiglitazone. Administration of this class of signaling mediators to *ob/ob* mice revealed that NO_2-FA lower insulin and glucose levels without inducing adverse side effects such as the increased weight gain induced by TZDs.

The rapidly expanding global burden of type II diabetes mellitus (DM)[3] and the concomitant increased risk for cardiovascular disease (1, 2) have motivated better understanding of relevant cell signaling pathways and potential therapeutic strategies. One major characteristic of metabolic syndrome and DM is insulin resistance, leading to hyperglycemia and dyslipidemia. Following initial clinical use of TZDs as anti-hyperglycemic agents to treat DM in the late 1990s, the nuclear receptor PPARγ was discovered as their molecular target. This receptor is expressed primarily in adipose tissue, muscle, and macrophages, where it regulates glucose uptake, lipid metabolism/storage, and cell proliferation/differentiation (3–5). Thus, PPARγ ligands and allied downstream signaling events play a pivotal role in both the development and treatment of DM (6, 7). This is underscored by the observation that mutations in the C-terminal helix 12 of the ligand-binding domain (LBD) of PPARγ (*e.g.* P467L or V290M) are linked with severe insulin resistance and the onset of juvenile DM (8).

The oxidizing inflammatory milieu contributing to the pathogenesis of obesity, diabetes, and cardiovascular disease also promotes diverse biomolecule oxidation, nitrosation, and nitration reactions by O_2 and $^{\bullet}NO$-derived species. Although oxidized fatty acids typically propagate proinflammatory conditions, the recently detected class of NO_2-FA act as anti-inflammatory mediators. Nitroalkene derivatives of oleic acid ($OA\text{-}NO_2$) and linoleic acid (LNO_2) have been detected in healthy human blood and murine cardiac tissue. The levels of free/unesterified $OA\text{-}NO_2$ are ~1–3 nM in human plasma (9, 10), with $OA\text{-}NO_2$ produced at increased rates and present at higher concentrations during inflammatory and metabolic stress (11–13). The signaling actions of NO_2-FA are primarily ascribed to the electrophilic olefinic carbon situated β to the electron-withdrawing NO_2 substituent, facilitating kinetically rapid and reversible Michael addition with nucleophilic amino acids (*i.e.* Cys and His) (14). NO_2-FA adduction of proteins and GSH occurs in model systems and clinically, with this reaction

* This work was supported, in whole or in part, by National Institutes of Health Grants R01 HL58115 and R01 HL64937 (to B. A. F.), P30 DK046204-15 and T32DK007052-34 (to M. P. C.), DK071662 and DK066202 (to H. E. X.), HL089301 (to H. E. X. and to Y. L.), and HL68878, HL089544, and HL75397. This work was also supported by The Hartwell Foundation (M. P. C.), American Diabetes Association Grant 7-08-JF-52 (to F. J. S.), American Heart Association Grants 0665418U (to F. J. S.) and 0840025N (to Y. E. C.), Deutsche Forschungsgemeinschaft (to T. K. R.), Deutsche Herzstiftung (to V. R.), and Jay and Betty Van Andel Foundation (to H. E. X.). B. A. F. acknowledges financial interest in Complexa, Inc.

[1] These authors contributed equally to this work.

[2] To whom correspondence should be addressed. E-mail: freerad@pitt.edu.

[3] The abbreviations used are: DM, diabetes mellitus; TZD, thiazolidinedione; PPARγ, peroxisome proliferator-activated receptor gamma; NO_2-FA, unsaturated fatty acid; DTT, dithiothreitol; LBDS, ligand-binding domain; $OA\text{-}NO_2$, nitro-oleic acid; LNO_2, linoleic acid; HPLC, high pressure liquid chromatography; MS/MS, tandem mass spectrometry; GST, glutathione *S*-transferase; BME, β-mercaptoethanol; ANOVA, analysis of variance; 15d-PGJ_2, 15-deoxyprostaglandin-J_2; Rosi, rosiglitazone; TR-FRET, time-resolved fluorescence resonance energy transfer.

influencing apparent blood and tissue concentrations (15). The adduction of nucleophilic amino acids in multiple signaling mediators alters protein function and patterns of gene expression. This results in the inhibition of macrophage activation via *S*-nitroalkylation of the NFκB p65 subunit (16), the inactivation the oxidant-generating enzyme xanthine oxidoreductase (17) *S*-nitroalkylation of Keap-1, activation of Nrf2-dependent phase 2 gene expression (18), and activation of heat shock factor-dependent gene expression (19). In addition to influencing the activities of these signaling mediators, OA-NO_2 and LNO_2 activate PPARγ (20). Although OA-NO_2 and LNO_2 transactivated PPARγ as potently as rosiglitazone (Rosi) in luciferase-based assay systems, NO_2-FA-induced differentiation of pre-adipocytes to adipocytes and subsequent triglyceride accumulation were diminished when compared with Rosi (20, 21). These results suggested that NO_2-FA may act as partial rather than full agonists of PPARγ and motivated more detailed investigation.

The large, relatively nonselective ligand binding pocket of PPARγ binds eicosanoids and oxidized fatty acid derivatives at micromolar concentrations (22), conferring to this receptor an ability to sense and transduce signals generated by an oxidizing inflammatory milieu that also supports the nitration of fatty acids. Most proposed "natural" PPARγ ligands are intermediates of lipid metabolism and oxidation that bind with low affinity at concentrations orders of magnitude greater than physiological conditions. Among these natural ligands are saturated and unsaturated free fatty acids (palmitic acid, K_d = 156 μM; and linoleic acid, K_d = 1 μM), prostaglandins (15-deoxyprostaglandin-J_2 (15d-PGJ_2), K_d ≈600 nM), leukotrienes, and other oxidized lipid derivatives (9- and 13 hydroxyoctadecadienoic acid, K_d = 10–20 μM; and epoxyeicosatrienoic acids, K_d = 1.1–1.8 μM), and lysophosphatidic acid (22). Synthetic TZD ligands, such as Rosi (K_d = 40–70 nM) (23, 24), bind PPARγ, increase insulin sensitivity (23), and alleviate symptoms associated with diabetes. Unfortunately, the full receptor activation of PPARγ by TZDs also results in undesirable side effects such as weight gain, edema, and an increase in adverse cardiovascular events (25, 26). Consequently, there is significant motivation to identify PPARγ agonists with gene expression activation profiles that differ from those of TZDs.

The possibility that NO_2-FA act as partial PPARγ agonists led us to investigate the biochemical mechanisms and consequences of PPARγ-NO_2-FA binding, as well as physiological outcomes upon chronic NO_2-FA treatment *in vivo*. We report herein the characterization of NO_2-FA binding and activation of PPARγ, the subsequent effects of NO_2-FA on PPARγ-coregulator interactions, and the ability of NO_2-FA to restore insulin sensitivity *in vivo*. Specifically, NO_2-FA covalently adduct PPARγ, display coregulator interactions distinct from those of Rosi, and reduce insulin and glucose levels in Lep^{ob} mice without inducing the weight gain typically induced by Rosi.

EXPERIMENTAL PROCEDURES

Materials—β-Mercaptoethanol was from Sigma. Sequencing grade modified trypsin was from Promega (Madison, WI). 15-d-PG J_2 and rosiglitazone were from Cayman Chemicals (Ann Arbor, MI). A purified synthetic peptide containing the NO_2-FA-reactive Cys-285 (IFQGCQFR) and identical to the predicted tryptic peptide upon PPARγ LBD digestion was prepared by the Peptide Synthesis Core Facility at the University of Pittsburgh.

NO_2-FA Synthesis, Detection, and Handling—NO_2-FA including OA-NO_2, LNO_2, and corresponding internal standards [$^{13}C_{18}$]OA-NO_2 and [$^{13}C_{18}$]LNO_2 were synthesized as described previously (21, 27, 28). NO_2-FA were synthesized via nitroselenation. In particular, oleic acid (NuCheck Prep, >99%) (29) was converted to a nitrophenyl selenylated intermediate in the presence of mercuric salts and then oxidized with hydrogen peroxide (30% aqueous) to yield the nitroalkene product OA-NO_2. The crude product was purified by multiple rounds of column chromatography on silica gel. The final product was analyzed for purity by ^{1}H NMR and HPLC-MS. OA-NO_2 produced by this method is an equimolar combination of 9- and 10-nitro-octadec-9-enoic acids. Specific OA-NO_2 regioisomers and allyl esters were synthesized and purified as described previously (27).

LC-MS Detection and Analysis of PPARγ Post-translational Modifications—First, 5 μg of purified human recombinant PPARγ LBD (residues 206–447, containing a His_6 tag) was incubated with ligands for 15 min in phosphate buffer, pH 7.4. PPARγ was then digested using mass spectrometry grade modified trypsin (Roche Applied Science) at a PPARγ to trypsin ratio of 50:1 overnight at 37 °C. The resulting peptide digest was immediately analyzed by HPLC-MS/MS for post-translational modification. Analyses were performed using an Agilent 1200 Series HPLC system (Agilent) coupled to an LTQ mass spectrometer (Thermo Fisher Scientific) equipped with an electrospray ionization source. HPLC was performed by injecting samples (3 μl) in a C18 reverse phase column (Zorbax SB 0.5-mm inner diameter, 0.5-μm particle size, and 150 mm, Agilent) at an 8 μl/min flow rate using 97% solvent A (H_2O, 0.1% formic acid) and 3% solvent B (acetonitrile, 0.1% formic acid). Peptides were eluted from the column using the following gradients: 7-min hold at 3% solvent B, and then the gradient was set to reach 65% solvent B in 50 min and then 100 in 1 min and hold at 100% solvent B for 5 min, and then re-equilibrated at initial conditions for 12 min. MS analysis was performed in the positive ion mode with the following source parameters that were optimized for the detection and identification of electrophilic fatty acid-modified cysteine- and histidine-containing peptides: source voltage 5 kV, capillary temperature 220 °C, tube lens 70 V, capillary voltage 50 V, and collision energy of 35 V. The covered PPARγ sequence (>90%) included all peptides containing either Cys or His residues (nucleophilic targets of nitroalkenes) (15), allowing for a comprehensive analysis of putative target residues. All modifications were further confirmed using [$^{13}C_{18}$]OA-NO_2-treated PPARγ. The ^{13}C-labeled modified peptides had the same retention times, confirming the detected *b* and *y* ions by a predicted mass shift of 18 *m*/*z*. All modified peptide spectral profiles were compared with respective nonmodified peptides and fragmentations further confirmed. Quantification of peptides using different concentrations of ligands was done using Excalibur QuanBrowser (Thermo Fisher Scientific). For quantification, the LTQ mass

TABLE 1

Mass spectrometric analysis of PPARγ electrophilic adduction

A, analysis of PPARγ tryptic digests. 5 μg of control and electrophilic lipid-treated PPARγ was trypsinized overnight or for 4 h and then subjected to HPLC-MS/MS using an LTQ mass spectrometer as detailed under "Experimental Procedures." Sequence in *green* shows peptides that were routinely identified. Initial analysis was performed using Bioworks 3.1. All peptides were manually confirmed. All peptides containing histidine and cysteine nucleophilic residues were detected. *B*, liquid chromatography-MS/MS characterization of peptides containing nucleophilic residues. Table 1 summarizes the retention time of the different peptides, theoretical mass, observed mass to charge ratio, and charge of the different peptides. Peptides derived from PPARγ treated with OA-NO_2 under the conditions used throughout the study show a significant shift in retention time due to increased hydrophobicity that was used as an additional confirmatory tool. *C*, analysis of Michael addition reaction between electrophilic fatty acid derivatives and nucleophilic residues in PPARγ. PPARγ (5 μg) was treated as indicated under "Experimental Procedures" with the different lipids at PPARγ/lipid ratios of 1.333, 0.133, and 0.022 for 15 min, trypsinized, and subjected to HPLC-MS/MS. The experiment was repeated three times at the different protein to lipid ratios, and the results summarized in this table. High represents modifications that were detected in all processed samples at all the different concentrations, with an extensive concomitant loss of native peptide. Medium represents peptides that were detected modified only at the higher concentrations of lipid used. Low represents peptides that were only detected modified in at least two separate experiments at only the highest concentrations of electrophile used with no significant loss of native peptide. Very low represents peptides that were found to be modified at the highest lipid concentrations of electrophile used with no loss of native peptide in at least one analysis. Integration of peak and calculation of peak areas was performed using Excalibur's QuanBrowser (Thermo Fisher).

A **PPARγ-LBD**

	1-10	11-20	21-30	31-40	41-50	51-60	61-70	71-80	81-90	91-100
200	PESAD	LRALAKHLYD	SYIKSFPLTK	AKARAILTGK	TTDKSPFVIY	DMNSLMMGED	KIKFKHITPL	QEQSKEVAIR	IFQGCQFRSV	EAVQEITEYA
300	KSIPGFVNLD	LNDQVTLLKY	GVHEIIYTML	ASLMNKDGVL	ISEGQGFMTR	EFLKSLRKPF	GDFMEPKFEF	AVKFNALELD	DSDLAIFIAV	IILSGDRPGL
400	LNVKPIEDIQ	DNLLQALELQ	LKLNHPESSQ	LFAKLLQKMT	DLRQIVTEHV	QLLQVIKKTE	TDMSLHPLLQ	EIYKDLY		

Green: MS-MS identified peptides
Red: non MS-MS covered peptides

Electrophile reactive residues, Cys 285 and His 217 / 323 / 449 / 266 / 425 / 466

B

				Observed			
Wild type PPAR LBD	RT (min)	Peptide	Mass (Da)	z	m/z	z	m/z
Native peptide	3.54	K.HITPLQEQSK.E	1180.63	2	590.82		
	23.15	K.LNHPESSQLFAK.L	1370.71	2	685.85		
	25.66	R.IFQGCQFR.S	998.49	2	499.74		
	30.88	K.KTETDMSLHPLLQEIYK.D	2046.06	3	682.69		
	30.76	R.QIVTEHVQLLQVIK.K	1647.98	2	824.99	3	549.99
	41.00	K.YGVHEIIYTMLASLMNK.D	1983.01	2	992.00	3	661.67
Modified Peptide treated with OA-NO_2	40.95	K.LNH*PESSQLFAK.L	1700.11	3	566.6		
	41.61	K.H*ITPLQEQSK.E	1508.03	2	754.52		
	45.06	R.QIVTEH*VQLLQVIK.K	1975.38	2	988.19	3	659.13
	46.25	R.IFQGC*QFR.S	1325.89	2	663.44		
	58.13	K.YGVH*EIIYTMLASLMNK.D	2310.41	3	770.80		

C

	PPARγ modification			
Peptide	OA-NO_2	LNO_2	Allyl-OA-NO_2	15d-PGJ_2
K.LNH*PESSQLFAK.L	Low	Low	Very Low	Not modified
K.H*ITPLQEQSK.E	Low	Low	Very Low	Not modified
R.QIVTEH*VQLLQVIK.K	Low	Low	Not modified	Not modified
R.IFQGC*QFR.S	High	High	Low	Medium/Low
K.YGVH*EIIYTMLASLMNK.D	Low	Low	Very Low	Not modified

spectrometer was set to continuously isolate and fragment the specific *m/z* values per period of the different peptides of interest (up to 15 ions per period). The most intense and characteristic *b* and *y* ions were selected and their areas integrated. The peptide FEFAVK derived from PPARγ trypsinization was chosen as an internal standard to account for processing, injection, and detection variability because it did not contain methionine, histidine, or cysteine and had good ionization and detection properties. The loss of native peptide was calculated by comparison with this standard peptide. In addition, the detection of the modified peptides was also analyzed.

Analysis and Quantification of BME Adducts—The analysis and quantification of BME-adducted molecules were performed using a hybrid triple quadrupole-linear ion trap mass spectrometer (4000 Q Trap, Applied Biosystems/MDS Sciex) in the multiple reaction monitoring scan mode (13). BME adducts of OA-NO_2 and [$^{13}C_{18}$]OA-NO_2 were detected by monitoring for molecules that undergo a $M^-/[M\text{-BME}]^-$ transition. The transitions used were 404.4/326.3 for BME-OA-NO_2 and

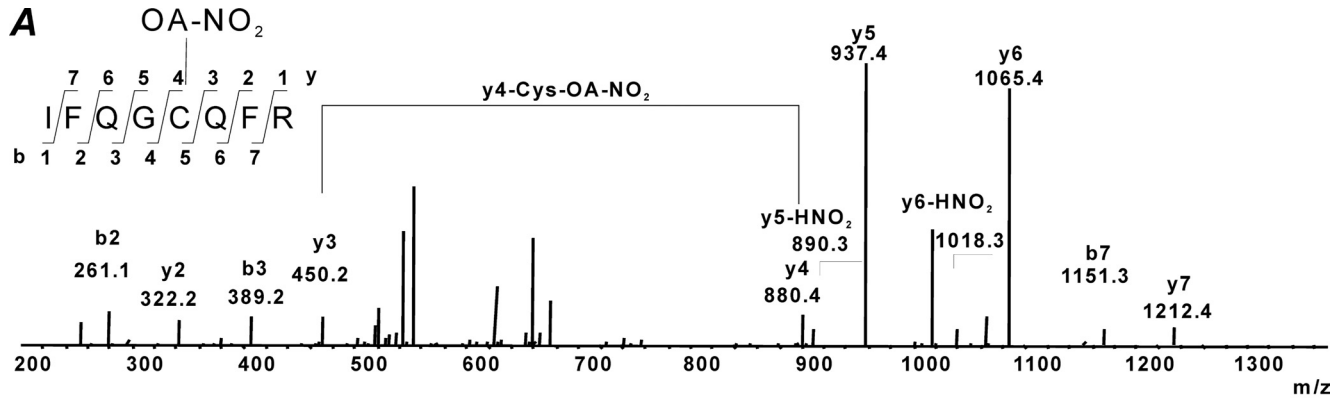

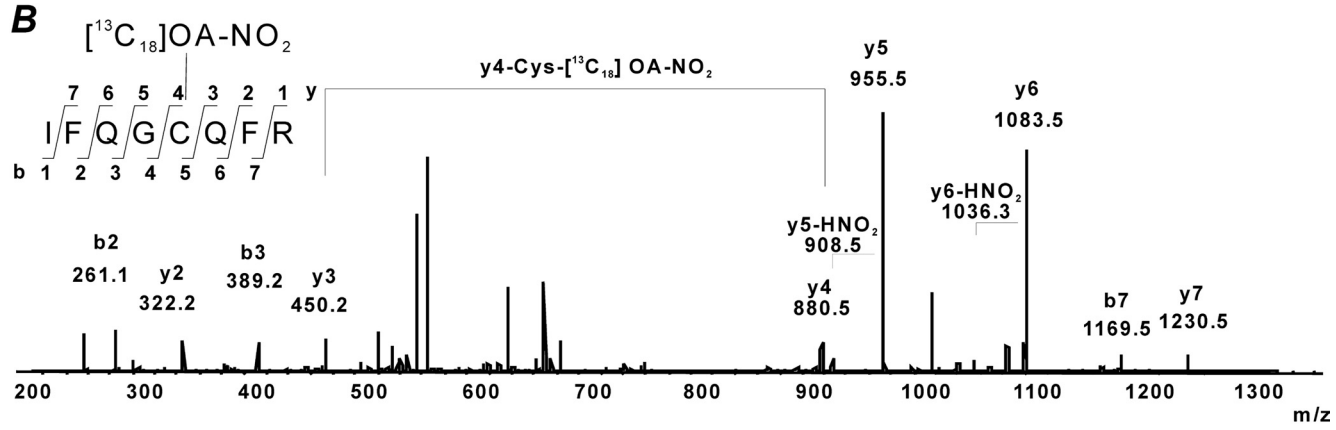

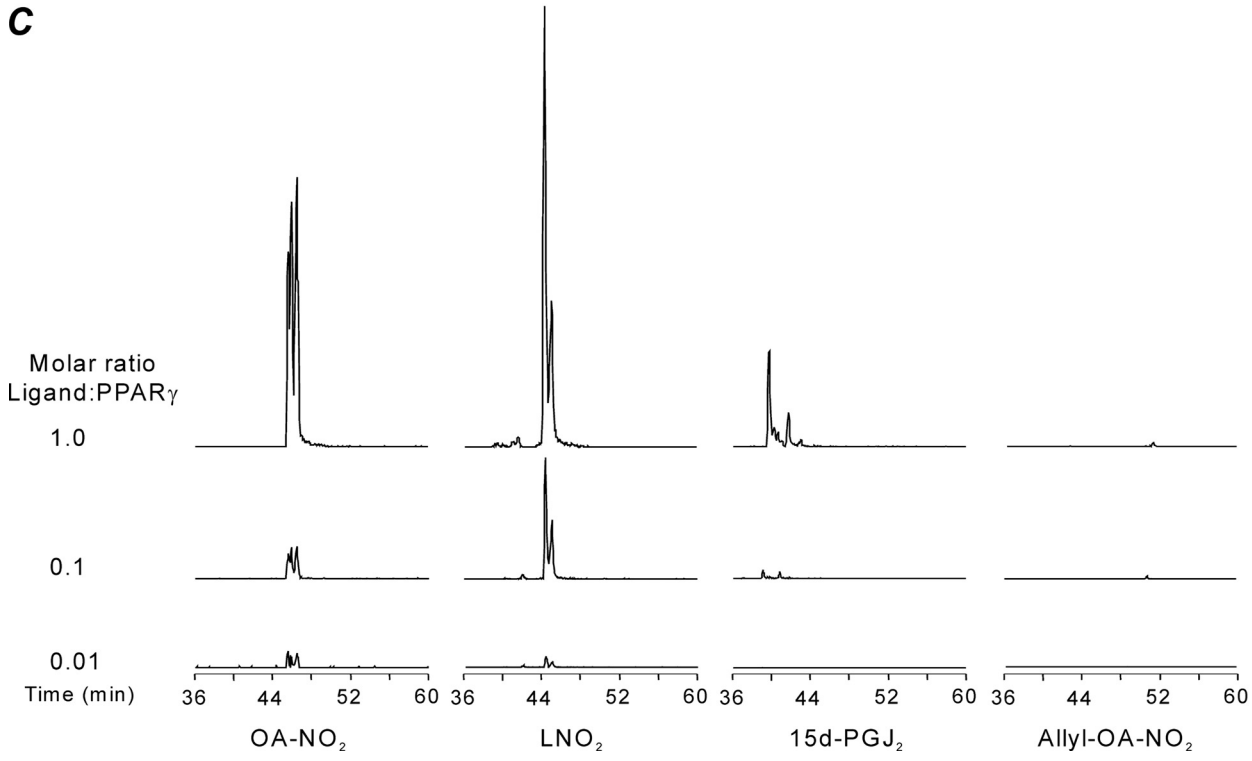

FIGURE 1. **Modification of PPARγ Cys-285 by electrophilic endogenous ligands.** *A,* OA-NO_2 covalently modifies Cys-285 in PPARγ. Fragmentation pattern of peptide IFQGCQFR was obtained from tryptic digest of OA-NO_2-treated PPARγ (*upper panel*). Synthetic peptide (IFQGCQFR) was adducted (nitroalkylated) *in vitro* using [$^{13}C_{18}$]OA-NO_2, and fragmentation pattern of PPARγ tryptic digested peptide was confirmed (*lower panel*). Peptides were resolved by reverse phase chromatography and analyzed by electrospray ionization-tandem mass spectrometry as detailed under "Experimental Procedures." *B,* PPARγ (5 μg) was incubated for 15 min in the presence of different ligands at the indicated molar ratios and then trypsinized. The chromatogram shows the formation of the specific OA-NO_2, LNO_2, and 15d-PGJ_2 adducted Cys-285 containing peptides. The ion trap mass spectrometer was set to trap the specific masses corresponding to the different adducted masses previously characterized (Pept-OA-$NO_2{}^{2+}$ *m/z* 663.4, Pept-$LNO_2{}^{2+}$ *m/z* 662.4, Pept-15d-$PGJ_2{}^{2+}$ *m/z* 657.9, and Pept-Allyl-OA-$NO_2{}^{2+}$ *m/z* 683.4). The chromatogram shows the sum of intensities of the following MS/MS ions for the different treatments $b_2{}^{+1} + b_3{}^{+1} + y_3{}^{+1} + y_5{}^{+1} + y_6{}^{+1} + y_7{}^{+2} + y_6{}^{+2}$.

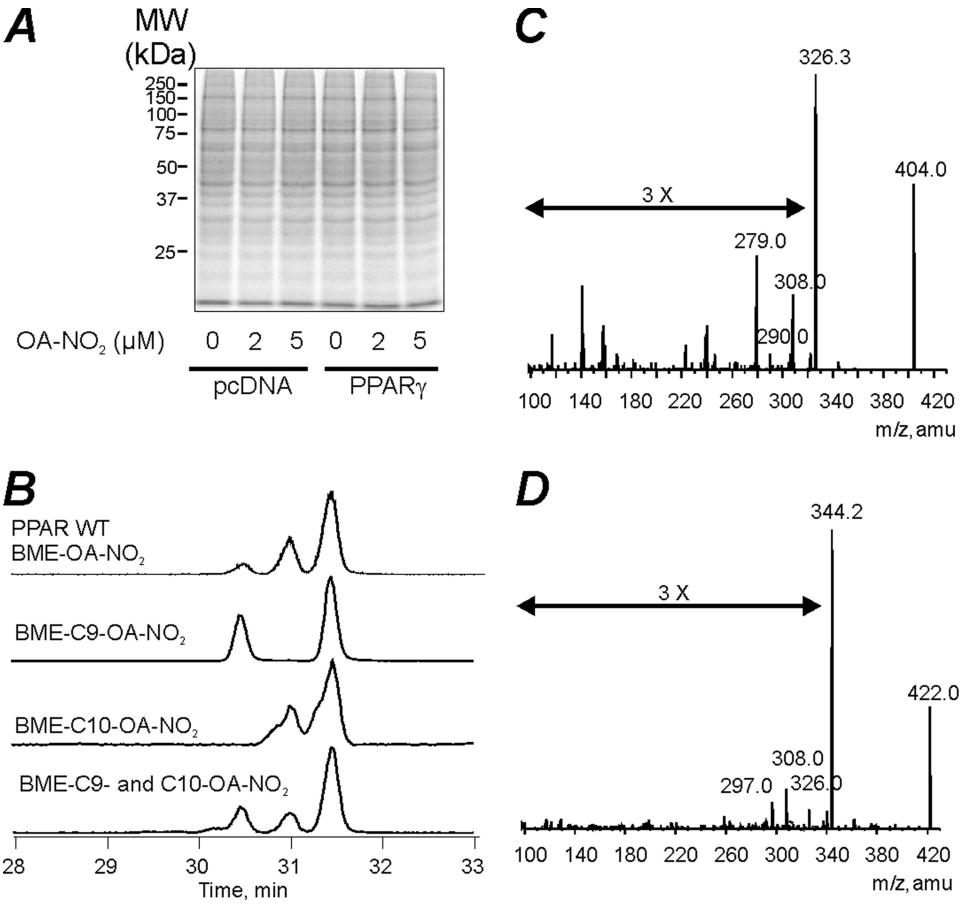

FIGURE 2. **OA-NO_2 covalently binds to the Cys-285 of PPARγ in HEK 293T cells.** *A,* Coomassie stain of protein gel electrophoresis of empty vector or PPARγ-transfected cells showed no change in net protein content or composition. *B,* chromatographic profile of BME-exchanged OA-NO_2 from immunoprecipitated wild type (WT) PPARγ (*top*), and the synthetic pure adducts of BME-9-OA-NO_2 (*2nd from top*), BME-10-OA-NO_2 (*3rd from top*), and an equimolar mixture of BME-9-OA-NO_2 and BME-10-OA-NO_2 (*bottom*). *C* and *D,* MS/MS confirmation of BME-OA-NO_2 and [$^{13}C_{18}$]BME-OA-NO_2 adducts obtained from chromatograms shown in *B*. The identity of the major fragments correspond to the loss of BME (−78 *m/z*), BME + H_2O (−96 *m/z*), BME + 2 H_2O (−114 *m/z*), and BME + HNO_2 (−125 *m/z*).

422.4/344.3 BME-[$^{13}C_{18}$]OA-NO_2. Samples were separated by reverse-phase HPLC using a 20 × 2-mm C18 Mercury MS column (3 μm, Phenomenex). OA-NO_2 adducts of BME were separated and eluted from the column using a gradient solvent system consisting of solvent A (H_2O containing 0.1% acetic acid) and solvent B (CH_3CN containing 0.1% acetic acid) at 750 μl/min under the following conditions: hold at 0% solvent B for 2 min, then 0–90% solvent B (3 min; hold for 2 min), and 90–0% B (0.1 min; hold for 2 min). The declustering potentials were −90 V and −50 V for GS-lipid and BME-lipid electrophilic adducts, respectively. The collision energies were set at −35 and −17 V for GS-lipid and BME-lipid electrophilic adducts, respectively. Zero grade air was used as source gas, and nitrogen was used in the collision chamber. Data were acquired and analyzed using Analyst 1.4.2 software (Applied Biosystems, Framingham, MA). Quantification was achieved by comparing peak area ratios between analytes and their corresponding internal standards, and analyte concentration was calculated using an internal standard curve. The isomeric distribution after covalent binding of OA-NO_2 to PPARγ and reaction with BME was analyzed and compared with pure 9-NO_2 and 10-NO_2 OA-NO_2 internal standards.

HEK 293T Cells—HEK 293T cells (ATCC, CRL-11268) were maintained in Dulbecco's modified Eagle's medium with high glucose supplemented with 10% fetal bovine serum (Hyclone) and grown at 37 °C in 5% CO_2. Cells were transiently transfected with 7 μg of pcDNA3 empty, FLAG-tagged PPARγ, or FLAG-tagged PPARγ C285A mutant expression vectors by calcium phosphate coprecipitation. The HEK 293T cells were then treated with different concentrations of OA-NO_2 for 2 h.

Immunoprecipitation—Cell lysates were prepared by washing with phosphate-buffered saline, and lysis was performed in TGH buffer (150 mM NaCl, 10 mM HEPES, 1 mM EDTA, 1 mM EGTA, 1% Triton X-100, and 10% glycerol) supplemented with protease inhibitors. Lysates were incubated with FLAG-agarose M2 beads (Sigma) at 4 °C overnight. Immunoprecipitation fractions were obtained by centrifugation at 14,000 × *g* for 1 min, washed with Tris-buffered saline three times, and then eluted with 3× FLAG peptides (Sigma) in Tris-buffered saline, pH 7.4, at 4 °C for 1 h. Supernatants, containing specific FLAG-tagged proteins, were assayed for NO_2-FA content via BME protein-to-BME trans-nitroalkylation reaction (13). Proteins were additionally resolved and quantified using the gel electrophoresis and silver staining (Invitrogen).

Immunoblotting—Total cell extracts or lysates were resolved on 10 or 11% SDS-PAGE and transferred onto nitrocellulose or polyvinylidene difluoride membranes (Bio-Rad) in Tris/glycine buffer (Bio-Rad). The membranes were probed with either monoclonal anti-FLAG M2 or polyclonal aP2 antibodies (Cell Signaling) and normalized using a polyclonal β-actin antibody (Sigma).

In Vitro Competitive Binding Studies—The GST-tagged PPARγ ligand-binding domain (PPARγ LBD), terbium-labeled anti-GST antibody, and Fluormone™ Pan-PPAR Green tracer were added to ligand in a black 384-well assay plate (Corning Glass catalog no. 677) for final assay concentrations of 5 nM PPARγ, 5 nM antibody, and 5 nM tracer. After a 1-h incubation at 25 °C, the terbium emission at 495 nm and the FRET signal at 520 nm were measured following excitation at 340 nm using a Tecan Ultra 384 microplate reader (Tecan Group Ltd., Maennedorf, Switzerland).

In Vitro Coactivator Recruitment Studies—The GST-tagged PPARγ ligand-binding domain (PPARγ LBD), terbium-labeled anti-GST antibody, and fluorescein-labeled peptide were added

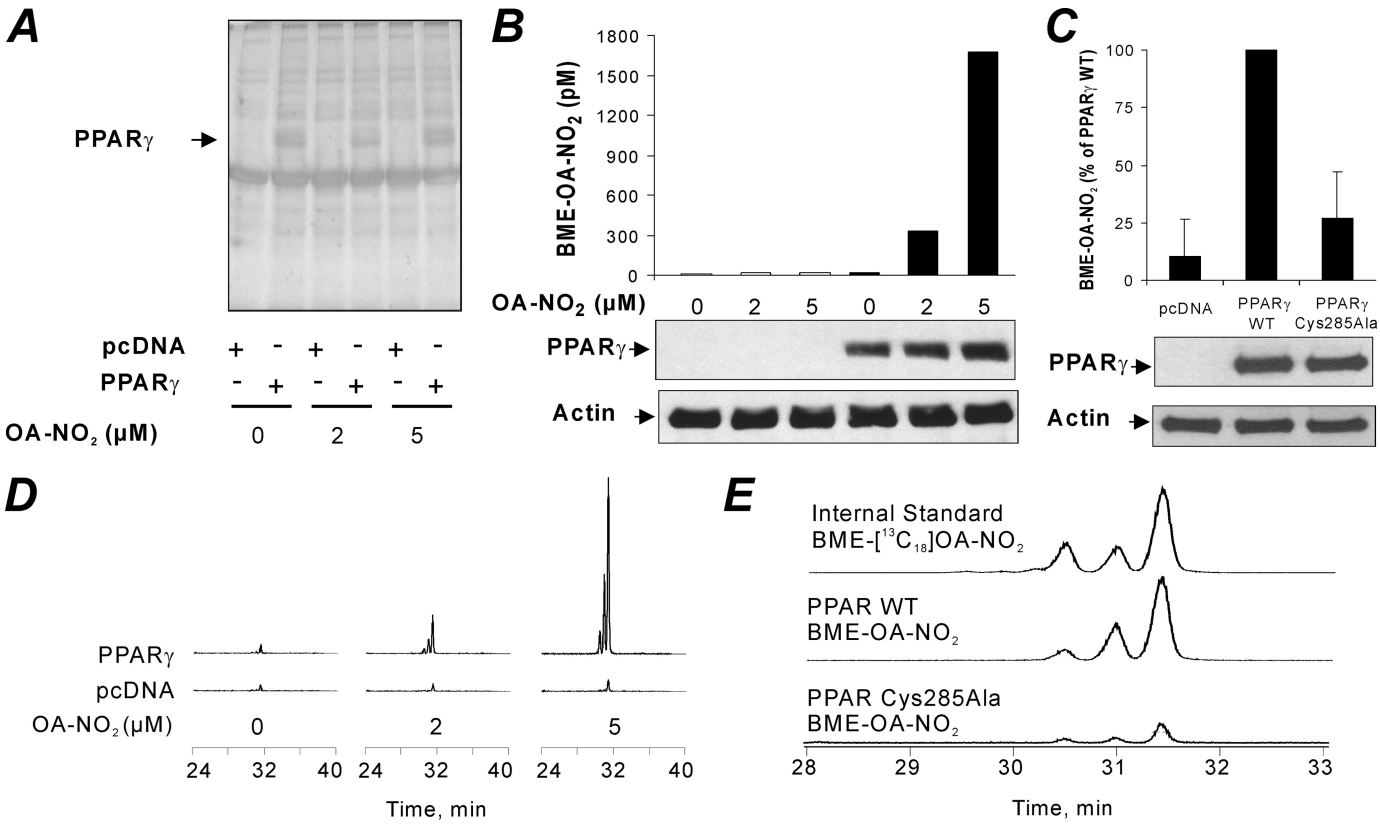

FIGURE 3. **OA-NO_2 covalently binds to the Cys-285 of PPARγ in HEK 293T cells in a regiospecific manner.** HEK 293T cells were transfected with PPARγ and treated with OA-NO_2. *A,* silver stain of FLAG-tagged PPARγ immunoprecipitated from transfected HEK 293T cells treated with 0, 2, and 5 μM OA-NO_2. Immunoprecipitated proteins were dissociated from beads using an excess of FLAG peptide, resolved by gel electrophoresis, and silver-stained. *B,* PPARγ-adducted OA-NO_2 was exchanged to BME from immunoprecipitated PPARγ in the presence of [$^{13}C_{18}$]OA-NO_2 internal standard and quantified by liquid chromatography-MS/MS as BME-OA-NO_2 (*upper panel*). *C,* BME-OA-NO_2 levels captured upon exchange to BME in immunoprecipitated lysates of empty vector, wild type (*WT*) PPARγ, and C285A mutant PPARγ-treated cells. BME exchange reactions were conducted in the presence of [$^{13}C_{18}$]OA-NO_2 internal standard and quantified by LC-MS-MS. The *lower panels* of *B* and *C* show controls for transfection efficiency (PPARγ Western blot) and loading controls (actin). *D,* chromatogram showing the BME adducts of OA-NO_2 following exchange reaction from the PPARγ receptor treated with different concentrations of OA-NO_2. *E,* chromatogram comparing [$^{13}C_{18}$]OA-NO_2 profiles with those of OA-NO_2 recovered with BME from wild type PPARγ and C285A mutant PPARγ cells.

to ligand in a black 384-well assay plate (Corning Glass catalog no. 3677) for final assay concentrations of 5 nM PPARγ, 5 nM antibody, and 125 nM peptide. For fold-change experiments, CBP-1, PGC-1α, TRAP/DRIP-2, NCoR ID2, and SMRT ID2 peptides (Invitrogen) were used at final assay concentrations of 500 nM. After a 2-h incubation at 25 °C, the terbium emission at 495 nm and the FRET signal at 520 nm were measured following excitation at 340 nm using a TECAN Ultra 384 microplate reader (Tecan Group Ltd., Maennedorf, Switzerland).

PPARγ Activation Reporter Assay—PPARγ-UAS-bla 293T division-arrested cells (Invitrogen) were used for the PPARγ reporter cell-based assay contained a PPARγ ligand-binding domain/GAL4 DNA-binding domain chimera stably integrated into a parental cell line previously engineered with a β-lactamase reporter gene under control of an upstream-activating sequence-response element. PPARγ-UAS-bla 293T division arrested cells were thawed and immediately plated in black-walled clear bottom and poly-D-lysine-coated 384-well plates at a density of 30,000 cells per well in assay medium (phenol red-free Dulbecco's modified Eagle's medium with 0.1% charcoal-stripped fetal bovine serum (Invitrogen)). Cells were then treated with serial dilutions of various ligands as indicated and incubated in a 37 °C and 5% CO_2 incubator for 18 h. Following incubation, LiveBLAzer^{TM}-FRET B/G loading solution (Invitrogen) was added to the cells, and they were incubated at room temperature for 2 h. Fluorescence intensity at 460 and 530 nm emission following excitation at 406 nm was measured using a TECAN Safire2 (Tecan Group Ltd., Maennedorf, Switzerland) with optimal gain settings determined by the instrument. After subtraction of fluorescence background from cell-free wells, the ratio of fluorescence intensity at 460 *versus* 530 nm (designated as 460:530 nm) was calculated. Data are expressed as mean ± S.D. and evaluated by a one-way ANOVA, post hoc Bonferroni test.

Pre-adipocyte 3T3-L1 Cell Studies—3T3-L1 cells were treated with OA, Rosi, OA-NO_2, or media alone and harvested after 3, 6, or 9 days. RNA was isolated using TRIzol (Invitrogen) and aP2 gene product amplified with Taqman probe Fabp4 (Applied Biosystems). 3T3-L1 cell differentiation was induced 2 days after confluence by incubating cells with Dulbecco's modified Eagle's medium and 10% fetal bovine serum (Hyclone) supplemented with 1 μM dexamethasone, 0.5 mM 1-methyl-3-isobutylxanthine, and 10 μg/ml insulin (DMI) ± agonist (3 μM Rosi, 3 μM OA, 3 μM OA-NO_2, 3 μM linoleic acid, or 3 μM LNO_2) for 3 days, after which cells were maintained with 10 μg/ml insulin ± agonist for an additional 2 days. At day 5, cells were cultured in Dulbecco's modified Eagle's medium, 10% fetal bovine serum ± agonist for an additional 2 days. RNA was

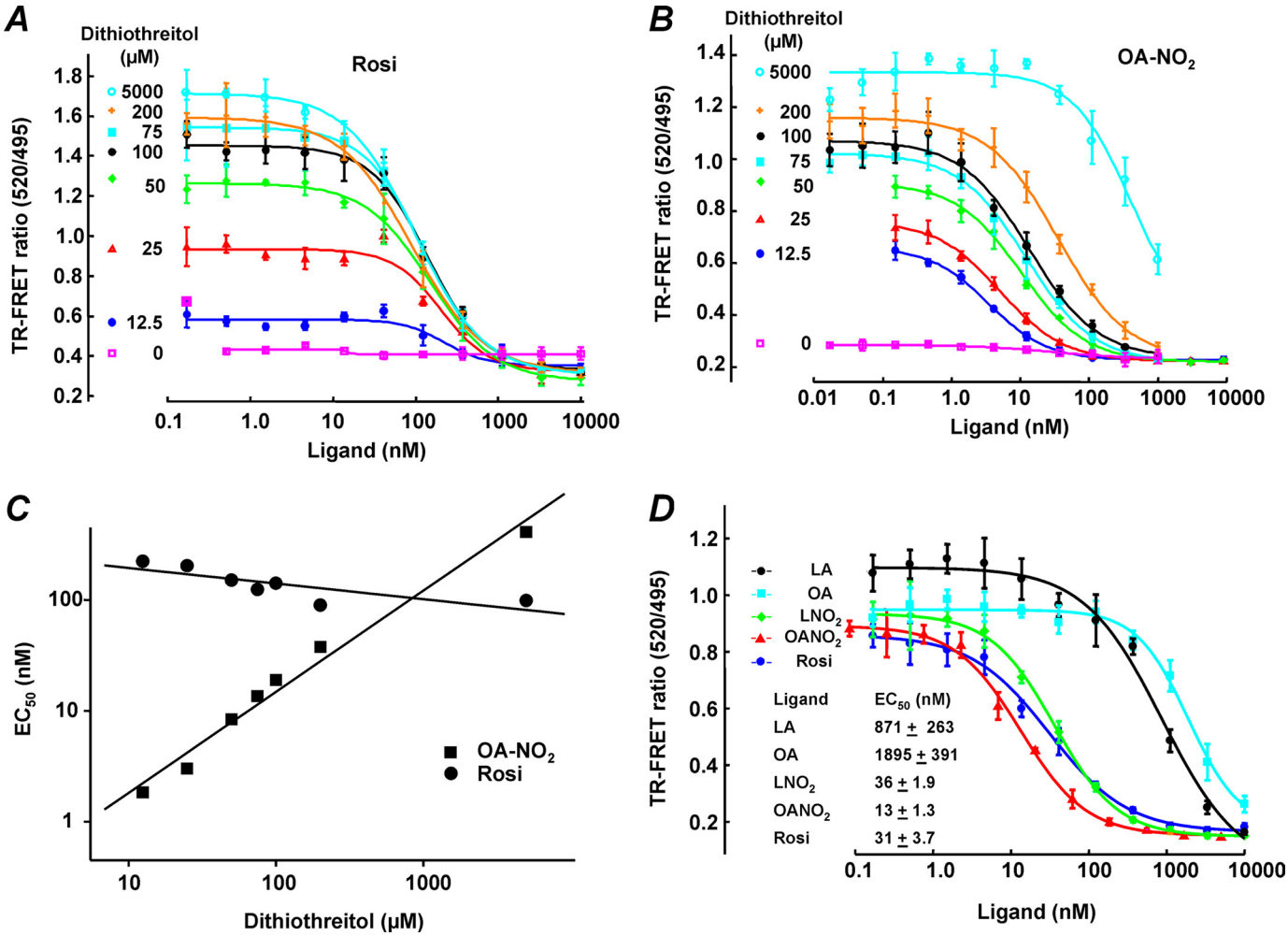

FIGURE 4. **PPARγ ligand activity of OA-NO_2, LNO_2, and rosiglitazone and the influence of dithiothreitol.** *A*, EC_{50} values for Rosi were determined by competitive binding analysis with concentrations of Rosi ranging from 0.17 to 10,000 nM. *B*, EC_{50} values for OA-NO_2 at varying concentrations of DTT were determined by competitive binding analysis with concentrations of OA-NO_2 ranging from 0.17 to 10,000 nM. *C*, EC_{50} values were plotted against DTT concentrations (12.5–5,000 μM) to determine the EC_{50} value of OA-NO_2 in the absence of reducing agent. Linear fitting equations are as follows: OA-NO_2, $Y = 0.91x - 0.65$, $r^2 = 0.99$, and Rosi, $Y = -0.14x + 2.43$, $r^2 = -0.801$. *D*, ligand binding curves were determined for linoleate, oleate, LNO_2, OA-NO_2, and Rosi with concentrations ranging from 0.17 to 10,000 nM in reactions containing 125 μM DTT. Curve-fitting equations and EC_{50} values were determined by XLfit4 and are displayed in the *inset*.

isolated from differentiated treated cells using TRIzol®, and complementary cDNA was generated. Quantitative real time PCR for GLUT4 and actin (GLUT4 forward, ATG AGA AAC GGA AGT TGG AGA GA; GLUT4 reverse, GTG GGT GCG GCT GCC; and actin forward, AGA GGG AAA TCG TGC GTG AC; actin reverse, CAA TAG TGA TGA CCT GGC CGT) were performed using the SYBR Green method. Expression of GLUT4 was compared with the housekeeping gene actin using the ΔΔ*Ct* method. For Oil Red O staining, cells were stained on day 7. Oil Red O images were collected by scanner and processed in Corel Photopaint by selecting circular areas representing 95% of the surface area of the plate to avoid edge effects (no adjustments to color, brightness/contrast, intensity, etc. were performed).

In Vivo Studies—All animal studies were approved by the University of Pittsburgh Institutional Animal Care and Use Committee (Approval 0905750). Osmotic mini-pumps (ALZET®, DURECT Corp., Cupertino, CA) containing either vehicle, OA (8 mg/kg/day), Rosi (6 mg/kg/day), or OA-NO_2 (8 mg/kg/day) were subcutaneously implanted in C57BL/6J and *Lep*^{ob} (*ob/ob*) male mice (for 28 days), 8–10 weeks of age (The Jackson Laboratories, Bar Harbor, ME), using isoflurane anesthesia. Food intake and mouse weight were monitored three times weekly. Blood glucose levels were assessed using a True Track glucometer (Home Diagnostics Inc., Ft. Lauderdale, FL). Insulin levels were measured via immunoassay (Alpco Diagnostics, Salem, NH). Tolerance tests, including oral glucose (2 mg/g body weight) on fasted mice (12–15 h), and intraperitoneal insulin (1.5 units/kg body weight) on nonfasted mice, were performed between 19 and 21 days of treatment, and blood samples were taken at various time points (0–120 min). Data are expressed as mean ± S.D., where asterisk is $p < 0.01$ (one-way ANOVA, post hoc Neuman-Keuls).

Statistical Analysis—All data were evaluated with a one-way ANOVA followed by the post hoc test indicated above. Data are expressed as means ± S.D.

RESULTS

Characterization of Covalent Modification of PPARγ by OA-NO_2—The PPARγ LBD was incubated in the absence and presence of different concentrations of OA-NO_2 at mole ratios

ranging from 1:1 to 1:100 (OA-NO_2/PPARγ) (Table 1*A*). At OA-NO_2/PPARγ mol ratios of 1:1, modifications of Cys-285, His-266, His-323, His-425 and His-449 were detected, although most histidines were modified at very low yields (Table 1, *B* and *C*). When the OA-NO_2/PPARγ ratio was lowered to 0.01, Cys-285 was the only residue undergoing covalent reaction with OA-NO_2. Overall, this indicates that histidines are minor targets for electrophilic fatty acids, and thus effects induced by peripheral alkylation reactions and conformational changes were considered negligible. The modification and fragmentation pattern of the Cys-285-containing peptide was further confirmed by comparison of the OA-NO_2-adducted PPARγ LBD tryptic peptide with a synthetic peptide adducted with either OA-NO_2 or [$^{13}C_{18}$]OA-NO_2 (Fig. 1*A*). The reactivity of Cys-285 toward electrophilic PPARγ agonists was then evaluated. We selected OA-NO_2 and LNO_2 as exemplary NO_2-FA, 15d-PGJ_2 as a representative α,β-unsaturated keto moiety, and OA-NO_2 having an allyl-adducted carboxylic acid as a negative control. The reactivity of 15d-PGJ_2 toward Cys-285 was much less than that of OA-NO_2. Moreover, the OA-NO_2 reactivity toward PPARγ-Cys-285 was similar to the one obtained for LNO_2 (Fig. 1*B* and Table 1C). These data are concordant with the lower K_i values displayed toward PPARγ by 15d-PGJ_2 compared with LNO_2 and OA-NO_2, as well as with the higher transactivation potency of NO_2-FA compared with 15d-PGJ_2. Moreover, PPARγ reactivity was (*a*) completely blocked by the allyl derivatization of OA-NO_2 (Fig. 1*B* and Table 1C), and (*b*) 10-nitro-octadec-9-enoic acid (C10-OA-NO_2) was more reactive toward the Cys-285 than 9-nitro-octadec-10-enoic acid (C9-OA-NO_2) (Fig. 2). Control studies did not support the possibility of postincubation adduction reactions or trans-nitroalkylation reactions during trypsinization for MS analysis. Short term trypsinization was also performed, and the results did not differ from longer incubations (data not shown).

Intracellular Modification of PPARγ by OA-NO_2—The cellular environment contains a high concentration of nucleophilic targets, including GSH and protein Cys and His residues. Although the reaction of NO_2-FA with nucleophiles is reversible, the cellular concentration of nucleophiles may act more as a sink rather than a reservoir of NO_2-FA. In addition, NO_2-FA are rapidly metabolized by mitochondria via β-oxidation (30). Thus, the uptake, transport, and binding of NO_2-FA to nuclear PPARγ can be limited by multiple competing cytosolic and nuclear reactions. To reveal whether NO_2-FA reach intracellular compartments and covalently modify and activate the receptor, HEK 293T cells were transfected with either empty vector or FLAG-PPARγ and treated with 0–5 μM OA-NO_2 for 2 h. PPARγ was immunoprecipitated from cell lysates, and the extent of thiol adduction was determined by HPLC-MS/MS upon exchange of the adducted electrophile to BME (13, 30). Expression levels of cellular proteins in general and PPARγ specifically were similar between different OA-NO_2 treatments and for cells transfected with a C285A mutant of PPARγ (Fig. 3, *A–C*, and Fig. 2*A*). Cell treatment with increasing concentrations of OA-NO_2 resulted in increased amounts of PPARγ-adducted OA-NO_2 that could be captured by an exchange reaction to BME (Fig. 3*B*). This was reflected by the appearance of PPARγ-derived BME-OA-NO_2 adducts (Fig. 3*D*). Cells transfected with C285A PPARγ lacking the electrophilic Cys-285 displayed nonspecific OA-NO_2 adduction that was similar to empty vector-transfected cells (Fig. 3*C*). Thus, in both *in vitro* and in cell models, PPARγ is a relevant target for low concentrations of OA-NO_2.

Characterization of OA-NO_2 Binding to PPARγ—TR-FRET analysis permitted more detailed characterization of ligand/receptor interactions. Using TR-FRET, the impact of covalent PPARγ adduction by NO_2-FA was analyzed, and competitive PPARγ LBD ligand displacement was quantified. GST-purified PPARγ LBD (0.5 nM) was incubated for 1 h with fluorescent ligand and the ligand of interest. Critical insight came from the use of different DTT concentrations in this analysis, as DTT is required in most ligand binding assays to maintain Cys-285 thiol reduction and receptor activity. Lowering DTT concen-

TABLE 2

Ligands that bind peroxisome proliferator-activated receptor γ covalently display decreasing EC_{50} values over time

Table indicates ligand binding curves for OA-NO_2, 9-OA-NO_2, 9-SA-NO_2, 12-SA-NO_2, Rosi, GW9662 (a ligand that binds PPARγ covalently), and OA with concentrations ranging from 0.17 to 10,000 nM and containing 125 μM DTT. Curve-fitting equations and EC_{50}s were determined by XLfit4.

	EC_{50} (nM)			
	3 min	10 min	20 min	1 hr
OA-NO_2	239	88	58	35
9-OA-NO_2	555	159	108	61
9-SA-NO_2	6795	8552	8358	8961
12-SA-NO_2	3023	2772	2290	1477
Rosi	17	24	28	44
GW9662	206	65	34	13
OA	7904	12066	13385	16118

TABLE 3

Comparison of rosiglitazone and OA-NO_2 modulation of coregulator interactions with PPARγ

Fold-changes in TR-FRET ratios (ligand/no ligand) were determined for the ligands Rosi (2 μM), and OA-NO_2 (2 μM) and for indicated coregulator peptides 62.5 nM.

	Fold Change			
Peptide ID	Rosiglitazone 2 μM	SD	$OANO_2$ 2 μM	SD
CBP-1	6.99	0.806	1.64	0.185
NCoRID2	0.53	0.062	0.68	0.029
PGC1a	2.55	0.201	1.25	0.165
PGC1b	1.69	0.143	0.99	0.041
TRAP220/DRIP2	7.46	0.563	1.73	0.069
SRC1-4	1.65	0.083	1.10	0.045
SMRTID2	0.60	0.033	0.90	0.040
TIF-1	1.24	0.166	0.96	0.114
DAX1-3	2.88	0.410	1.41	0.086
EA2	1.30	0.154	1.10	0.049
EAB1	1.26	0.068	1.01	0.044
PRIP/Rap250	2.15	0.219	1.18	0.087
LCoR	1.58	0.064	1.00	0.045
NCoRID1	0.92	0.067	0.99	0.075
NSD1	1.12	0.033	0.99	0.075
RIP-140 L6	2.45	0.064	1.12	0.110

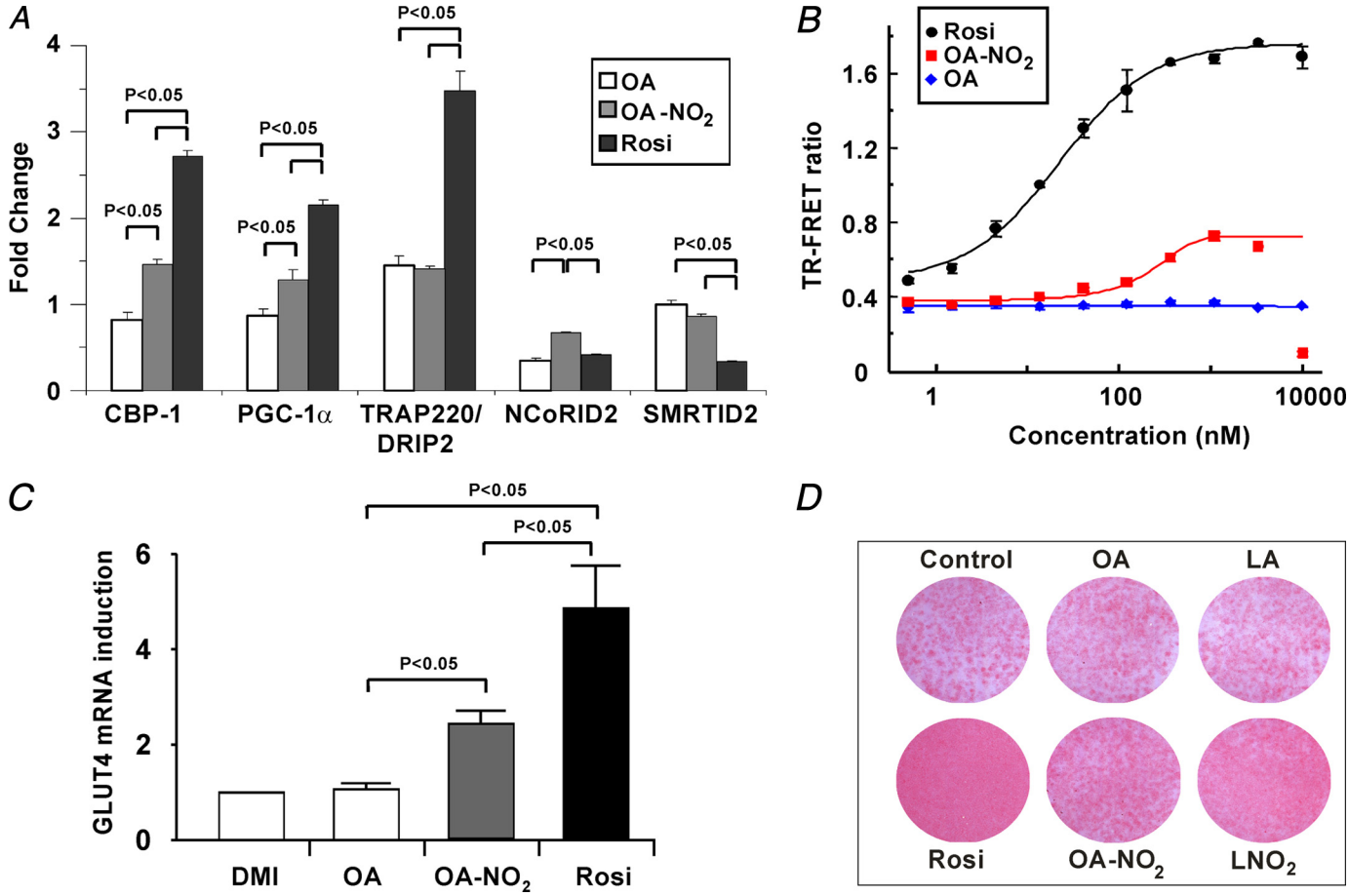

FIGURE 5. **OA-NO_2 is a partial agonist of PPARγ.** *A*, fold-change in TR-FRET ratios (ligand/no ligand) was determined for the ligands Rosi (5 μM), OA (20 μM), and OA-NO_2 (5 μM) and for indicated coregulator peptides. Ligand concentrations were utilized that induced maximum receptor occupancy as reflected by fluorescent reporter-ligand displacement. Statistics were calculated by a one-way ANOVA (post hoc Tukey). *B*, PPARγ β-lactamase reporter assays for Rosi, OA, and OA-NO_2 with concentrations ranging from 0.5 to 10,000 nM. Curve-fitting equations were determined by XLfit4. *C*, *Glut4* gene expression in 3T3-L1 adipocytes differentiated with DMI ± 3 μM agonist (day 8). Data are expressed as mean ± S.D. and evaluated by a one-way ANOVA, post hoc Tukey test. *D*, Oil Red-O staining of 3T3-L1 adipocytes differentiated with DMI ± 3 μM agonist (day 7).

tration decreased the assay window for Rosi (Fig. 4*A*) and revealed that DTT competitively reacts with added NO_2-FA, resulting in a right shift of EC_{50} with increasing DTT concentrations (Fig. 4*B*). Thus, measuring EC_{50} values for ligands at varying DTT concentrations allowed extrapolation of an EC_{50} value for OA-NO_2 of <1 nM in the absence of DTT (Fig. 4*C*). For comparing various ligands, 125 μM DTT was uniformly used, with an appreciation that actual EC_{50} values of PPARγ for electrophilic fatty acids can still be >10-fold less than observed (OA-NO_2 and LNO_2, 13 and 36 nM, respectively, and Rosi, 31 nM, see Fig. 4*D*). The EC_{50} values of oleic acid and linoleic acid were 1900 and 870 nM, respectively.

The adduction of OA-NO_2 with the LBD was also studied in the context of the competitive binding of ligands. The covalent nature of NO_2-FA binding should result in a left-shift of the EC_{50} value over time, as more and more of the receptor becomes adducted. GST-purified PPARγ LBD (0.5 nM) was incubated with fluorescent ligand and the ligand of interest, and then terbium emission and FRET signals were measured at various times during reactions (3, 10, 20, and 60 min). This revealed a decreased EC_{50} value over time for OA-NO_2, indicating that the dissociation rate of OA-NO_2 from PPARγ is much lower than for Rosi or the nonelectro-

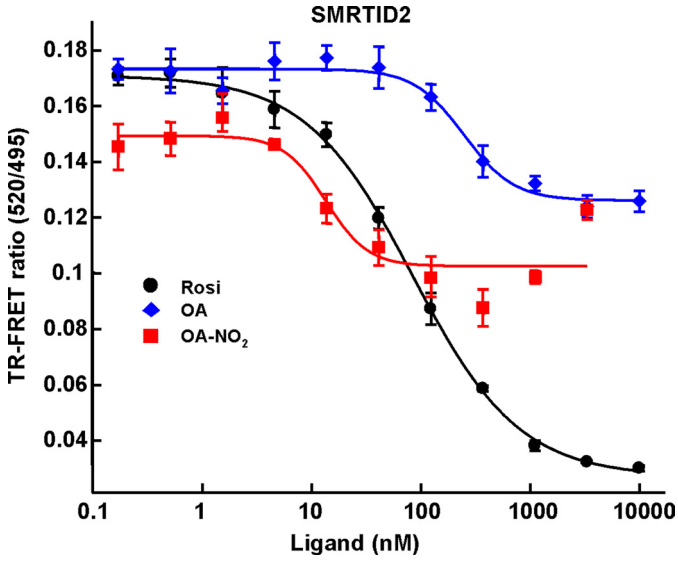

FIGURE 6. **Ligand titration curve for SMRT ID2 coregulator peptide indicate that OA-NO_2 is a partial agonist of PPARγ.** TR-FRET ratios for the coregulator SMRT ID2 peptide and the indicated ligands Rosi, OA, and OA-NO_2. Curve-fitting equations were determined by XL-fit.

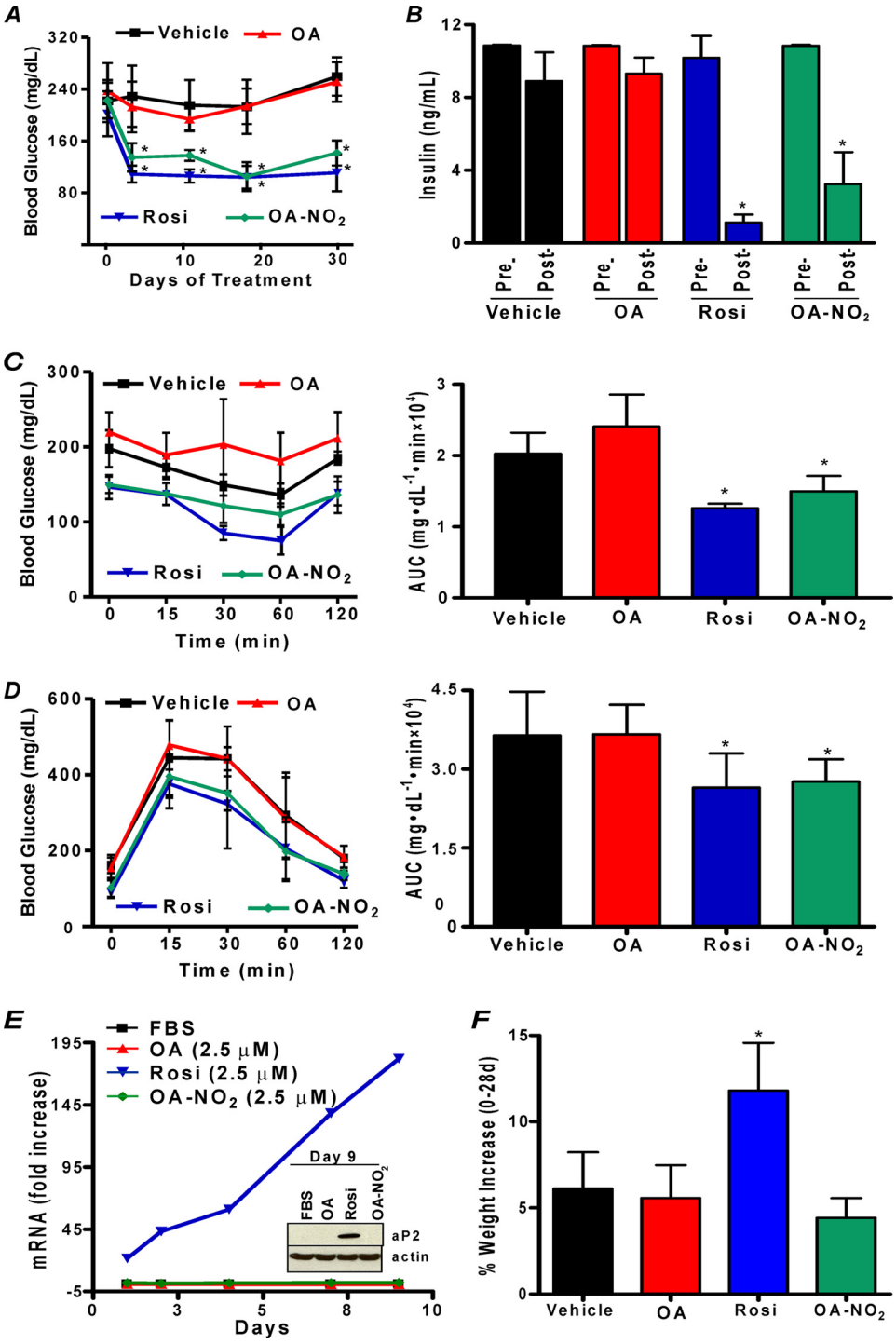

FIGURE 7. **$OA\text{-}NO_2$ exhibits antidiabetic and antiadipogenic effects *in vivo*.** $OA\text{-}NO_2$ lowers glucose within 4 days of pump implantation (day 0) (*A*) and restores insulin sensitivity in leptin-deficient diabetic *Lep*^{ob} (*ob/ob*) mice 28 days (*post-*) following pump implantation (day 0, *pre-*). Insulin administration to $OA\text{-}NO_2$-treated mice produces a rapid decrease in glucose compared with vehicle and oleate-treated mice (*left* and *right panels*) (*C*). Insulin sensitivity was significantly improved in $OA\text{-}NO_2$-treated mice following oral glucose administration (*right* and *left panels*) (*D*). Rosi treatment activates aP2 gene expression in 3T3-L1 cells (*E*) and induces significant weight gain in *ob/ob* mice (*F*). Data are expressed as means ± S.D., where *asterisk* indicates $p < 0.01$ (one-way ANOVA, post hoc Neuman-Keuls).

philic homolog of $OA\text{-}NO_2$, nitro-stearic acid (Table 2). This significant time-dependent reduction in NO_2-FA EC_{50}, compared with ligands that lack electrophilic reactivities (Rosi, oleic acid, and nitro-stearic acid), further affirmed the covalent interaction of $OA\text{-}NO_2$ with PPARγ.

$OA\text{-}NO_2$ Is a Selective PPARγ Modulator—TR-FRET-based analysis of >20 coregulator peptides indicated that PPARγ binding by $OA\text{-}NO_2$ induces few of the changes in coregulator peptide interactions typically induced by Rosi, supporting a role for NO_2-FA as partial agonists of PPARγ (Table 3). Significant coregulator peptide binding changes were observed for peptides derived from the following coregulators (Fig. 5*A*): cAMP-response element-binding protein-binding protein, motif 1 (CBP-1), thyroid hormone receptor-activated protein 220, also known as VDR-interacting protein, motif 2 (TRAP220/DRIP-2), PPARγ coactivator 1α (PGC-1α), nuclear corepressor protein interacting domain 2 (NCoR ID2), and the silencing mediator of retinoid and thyroid hormone receptors, interacting domain 2 (SMRT ID2) (Fig. 5*A*). In contrast to Rosi, which both strongly recruits the coactivator peptides of CBP-1, TRAP220/DRIP-2, and PGC-1α and strongly displaces the corepressors NCoR ID2 and SMRT ID2, $OA\text{-}NO_2$ induced a weaker recruitment and displacement of coregulator peptides, indicating a partial PPARγ agonist activity (Fig. 5*A*). This partial agonist behavior of $OA\text{-}NO_2$ is also exemplified by the lower extent of SMRT ID2 displacement that is induced by $OA\text{-}NO_2$ compared with Rosi (Fig. 6). The modified PPARγ interaction with coregulators is further confirmed by the partial agonism induced by NO_2-FA in a cell-based reporter assay using the chimeric Gal4 DNA-binding domain fused to the LBD of PPARγ with a β-lactamase reporter (Fig. 5*B*). The EC_{50} value of NO_2-FA for receptor activation is considerably lower than for Rosi, with potency in the low nanomolar range. The partial agonism of $OA\text{-}NO_2$ observed in this test system is also supported by analysis of PPARγ ligand-induced preadipocyte differentiation to adipocytes. $OA\text{-}NO_2$ induced Glut4 expression (Fig. 5*C*), and at the same time induced less adiponectin expression (data not shown) and triglyceride accumulation than that induced by Rosi (Fig. 5*D*), again supporting partial agonist activity of NO_2-FA.

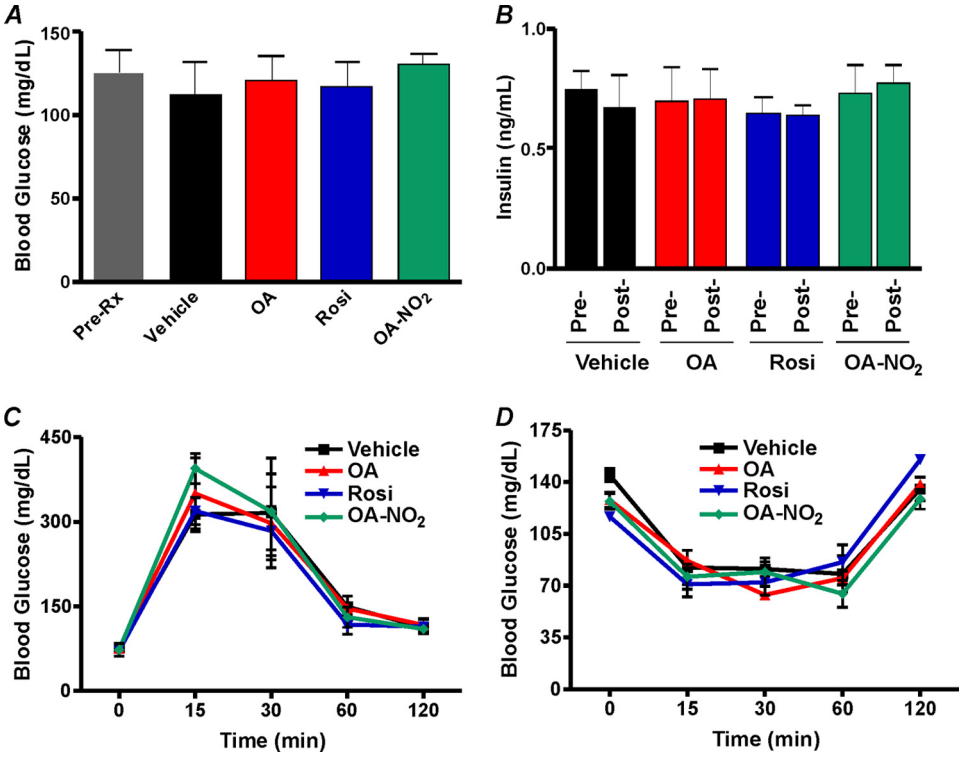

FIGURE 8. **OA-NO_2- and Rosi-treated nondiabetic mice are normoglycemic and respond normally to administered insulin and glucose.** Blood glucose (*A*) and insulin levels (*B*) were unaffected by vehicle, OA, Rosi, or OA-NO_2 treatment in age-matched, anti-diabetic wild type mice. Oral glucose (*C*) and intraperitoneal insulin (*D*) tolerance tests reveal that treatment groups (vehicle, OA, Rosi, or OA-NO_2) do not vary in age-matched, wild type C57BL/6J mice. Data are expressed as mean ± S.D.

OA-NO_2 Normalizes Hyperglycemia in Diabetic Mice—Diabetic *ob/ob* mice are obese and severely insulin-resistant. Moreover, TZDs such as Rosi exert PPARγ-mediated anti-hyperglycemic effects in *ob/ob* mice but display adverse side effects such as accelerated weight gain (31). The selective modulator actions of OA-NO_2 were tested *in vivo* for anti-hyperglycemic activity and possible side effects. Administration of 8 mg/kg OA-NO_2 via an osmotic mini-pump over a period of 4 weeks gave a mean plasma level of 32.2 ± 4.5 nM OA-NO_2 in obese *ob/ob* mice. OA-NO_2 significantly normalized blood glucose levels within 4 days of pump implantation, comparable with those induced by Rosi (Fig. 7*A*). Insulin levels, a hallmark of type II DM, were also significantly reduced by Rosi and OA-NO_2 but not by vehicle or native oleic acid administration (Fig. 7*B*). There were no changes in blood glucose or insulin levels in all treatment groups of nondiabetic wild type C57BL/6J mice (Fig. 8). Insulin resistance in vehicle and oleate-treated *ob/ob* mice was confirmed by intraperitoneal insulin and oral glucose tolerance tests. In contrast, intraperitoneal insulin administration in OA-NO_2-treated mice revealed a significant and rapid decrease in glucose levels compared with vehicle and oleate treatments (Fig. 7*C, right* and *left panels*). Notably, Fig. 7*D* shows improved insulin sensitivity when glucose is administered orally in OA-NO_2-treated mice (compared with vehicle and oleate treated mice). Insulin and glucose tolerance tests showed no changes in treated groups in non-insulin-resistant wild type C57BL/6J mice (Fig. 8). An adverse side effect of Rosi, weight gain, reflects both edema and adipogenesis. OA-NO_2-treated mice did not gain weight at rates greater than vehicle and native fatty acid controls, as opposed to Rosi-treated mice (Fig. 7*F*), with all groups having similar caloric intakes (data not shown). In 3T3-L1 adipocytes, Rosi but not OA-NO_2 stimulated RNA transcription and translation of the PPARγ-regulated gene, aP2 (Fig. 7*E*). This fatty acid trafficking protein mediates early and late stages of adipogenesis, affecting adipocyte number and triglyceride content. This difference in aP2 expression is consistent with the observation that Rosi induced greater extents of adipocyte lipid accumulation than OA-NO_2 (Fig. 5*D*).

DISCUSSION

The crystallographic analysis of LNO_2 bound to the PPARγ pocket revealed close proximity between the electrophilic carbon β to the nitro group and Cys-285 (32). This spatial arrangement motivated a more detailed examination of the interactions of NO_2-FA with PPARγ. It has been previously reported that 15d-PGJ_2 reacts covalently with Cys-285 *in vitro*, inducing a particular nuclear receptor conformational change (33). More recently, the covalent modification of PPARγ Cys-285 was shown to lead to unique receptor conformational changes that resulted in differential regulation of downstream gene transcription (34). Of relevance, the interaction and alkylation of nucleophilic residues distal to the binding pocket may induce additional conformational changes that result in unique coregulator associations and interactions. Thus, as a first approach to defining the mechanism of PPARγ activation by nitroalkene fatty acid derivatives, the nucleophilic amino acids of PPARγ that react with nitrated fatty acids were identified. The results from this approach reinforced the concept that the environment of Cys-285 renders it very electrophile-reactive, probably by reducing the pK_a of the thiol and favoring the thiolate anion. This also suggests that additional stabilization of a covalent ligand-receptor complex can occur and has important implications for the pharmacokinetics of PPARγ-dependent cell signaling when the receptor is covalently adducted by ligand.

PPARγ activation by full agonists such as Rosi induces the expression of proteins that regulate cell differentiation, lipid trafficking, glucose metabolism, and inflammation, thus increasing insulin responsiveness and decreasing blood glucose. However, full PPARγ agonists also stimulate adipocyte differentiation *in vitro* and induce weight gain *in vivo*, motivating a search for selective modulators that activate a subset of PPARγ-regulated genes with reduced side effects (7, 35). Here, we reveal that electrophilic NO_2-FA derivatives, products of the oxidizing and nitrating conditions promoted by inflammation,

bind to and react avidly with the redox-sensitive LBD Cys-285 of PPARγ (Fig. 3). This NO_2-FA adduction may also serve to protect the oxidation-sensitive Cys-285 of the LBD from inflammatory-derived reactive species. These data reinforce the potent and unique nature of PPARγ binding by NO_2-FA. TZDs bind and activate PPARγ reversibly through both hydrophobic and hydrogen bonding interactions (36). In contrast, electrophilic NO_2-FA bind and activate PPARγ by not only hydrophobic and hydrogen bonding interactions but also by covalent reaction with the nucleophilic LBD Cys-285, a scenario where saturation binding kinetics no longer apply.

The specific ligand, cell type, and cell signaling conditions all combine to define the available coregulatory protein pool that interacts with PPARγ. Hundreds of coregulator proteins have been identified that are either protein-modifying enzymes or scaffolds for transcriptional machinery that promote (coactivators) or prevent (corepressors) transcription. Ligand-dependent coregulator protein recruitment dictates the specificity of transcriptional responses that in turn lead to changes in metabolic homeostasis. Notably, coregulators are also pharmacological targets being pursued as modulators of metabolic adaptation. Rosi recruits and displaces a specific pattern of coregulators upon PPARγ binding, inducing a biological response characteristic of full PPARγ agonists. In contrast, binding of partial agonists induces a modified coregulator-PPARγ interaction pattern that differentially transactivates target genes (37). Although OA-NO_2 and Rosi both bind PPARγ with high affinity, distinctively different coregulator protein interactions result. This crucial aspect of ligand-specific receptor conformation and subsequent patterns of transcriptional complex assembly, receptor-DNA binding, and gene expression lends a second level of specificity to PPARγ signaling and defines how a particular ligand influences downstream events such as adipocyte differentiation, lipid metabolism, renal fluid regulation, and cellular bioenergetics (38–42). PPARγ agonism by electrophilic NO_2-FA manifests unique binding kinetics and induces conformational changes in PPARγ that result in coregulator interactions unique to these inflammatory by-products. These properties suggest that NO_2-FA might induce physiological responses that differ from Rosi (22, 32, 36, 37). These findings also support that the pro-adipogenic actions of Rosi, *i.e.* fat accumulation, can be linked in part to characteristic recruitment of the coactivators TRAP220/DRIP-2 and CBP-1. Related to this, the weak corepressor displacement (NCoR ID2 and SMRT ID2) by OA-NO_2 may result in inhibition of adipogenesis (39).

In summary, this is the first demonstration of NO_2-FA adduct formation with PPARγ and *in vivo* evidence for NO_2-FA as anti-hyperglycemic agents that favorably modulate adipogenesis and circumvent the accelerated weight gain associated with TZD administration. The presence of endogenous NO_2-FA in healthy human plasma at nanomolar levels and the increased formation of fatty acid nitration products during metabolic and inflammatory stress (11, 13) underscore the potential ability of NO_2-FA to modulate PPARγ signaling. Plasma levels of ~30 nM *in vivo* were sufficient to result in a pharmacological effect. This selective PPARγ ligand property of NO_2-FA is also borne out by cell and receptor-coregulatory protein interaction studies. Inasmuch as cardiovascular disease incidence is increased in the diabetic population and TZD-based PPARγ agonists increase risk for adverse cardiovascular events, the unique PPARγ interactions of electrophilic fatty acids encourage further model systems and clinical investigation.

REFERENCES

1. Cerghizan, A., Bala, C., Nita, C., and Hancu, N. (2007) *Exp. Clin. Cardiol.* **12,** 83–86
2. Hajer, G. R., van Haeften, T. W., and Visseren, F. L. (2008) *Eur. Heart J.* **29,** 2959–2971
3. Tontonoz, P., and Spiegelman, B. M. (2008) *Annu. Rev. Biochem.* **77,** 289–312
4. Altiok, S., Xu, M., and Spiegelman, B. M. (1997) *Genes Dev.* **11,** 1987–1998
5. Ricote, M., Li, A. C., Willson, T. M., Kelly, C. J., and Glass, C. K. (1998) *Nature* **391,** 79–82
6. Guilherme, A., Virbasius, J. V., Puri, V., and Czech, M. P. (2008) *Nat. Rev. Mol. Cell Biol.* **9,** 367–377
7. McGuire, D. K., and Inzucchi, S. E. (2008) *Circulation* **117,** 440–449
8. Barroso, I., Gurnell, M., Crowley, V. E., Agostini, M., Schwabe, J. W., Soos, M. A., Maslen, G. L., Williams, T. D., Lewis, H., Schafer, A. J., Chatterjee, V. K., and O'Rahilly, S. (1999) *Nature* **402,** 880–883
9. Tsikas, D., Zoerner, A., Mitschke, A., Homsi, Y., Gutzki, F. M., and Jordan, J. (2009) *J. Chromatogr. B Analyt. Technol. Biomed. Life Sci.* **877,** 2895–2908
10. Tsikas, D., Zoerner, A. A., Mitschke, A., and Gutzki, F. M. (2009) *Lipids* **44,** 855–865
11. Rudolph, V., Rudolph, T. K., Schopfer, F. J., Bonacci, G., Woodcock, S. R., Cole, M. P., Baker, P. R., Ramani, R., and Freeman, B. A. (2010) *Cardiovasc. Res.* **85,** 155–166
12. Freeman, B. A., Baker, P. R., Schopfer, F. J., Woodcock, S. R., Napolitano, A., and d'Ischia, M. (2008) *J. Biol. Chem.* **283,** 15515–15519
13. Schopfer, F. J., Batthyany, C., Baker, P. R., Bonacci, G., Cole, M. P., Rudolph, V., Groeger, A. L., Rudolph, T. K., Nadtochiy, S., Brookes, P. S., and Freeman, B. A. (2009) *Free Radic. Biol. Med.* **46,** 1250–1259
14. Baker, L. M., Baker, P. R., Golin-Bisello, F., Schopfer, F. J., Fink, M., Woodcock, S. R., Branchaud, B. P., Radi, R., and Freeman, B. A. (2007) *J. Biol. Chem.* **282,** 31085–31093
15. Batthyany, C., Schopfer, F. J., Baker, P. R., Durán, R., Baker, L. M., Huang, Y., Cerveñansky, C., Branchaud, B. P., and Freeman, B. A. (2006) *J. Biol. Chem.* **281,** 20450–20463
16. Cui, T., Schopfer, F. J., Zhang, J., Chen, K., Ichikawa, T., Baker, P. R., Batthyany, C., Chacko, B. K., Feng, X., Patel, R. P., Agarwal, A., Freeman, B. A., and Chen, Y. E. (2006) *J. Biol. Chem.* **281,** 35686–35698
17. Kelley, E. E., Batthyany, C. I., Hundley, N. J., Woodcock, S. R., Bonacci, G., Del Rio, J. M., Schopfer, F. J., Lancaster, J. R., Jr., Freeman, B. A., and Tarpey, M. M. (2008) *J. Biol. Chem.* **283,** 36176–36184
18. Villacorta, L., Zhang, J., Garcia-Barrio, M. T., Chen, X. L., Freeman, B. A., Chen, Y. E., and Cui, T. (2007) *Am. J. Physiol. Heart Circ. Physiol.* **293,** H770–H776
19. Kansanen, E., Jyrkkänen, H. K., Volger, O. L., Leinonen, H., Kivelä, A. M., Häkkinen, S. K., Woodcock, S. R., Schopfer, F. J., Horrevoets, A. J., Ylä-Herttuala, S., Freeman, B. A., and Levonen, A. L. (2009) *J. Biol. Chem.* **284,** 33233–33241
20. Schopfer, F. J., Lin, Y., Baker, P. R., Cui, T., Garcia-Barrio, M., Zhang, J., Chen, K., Chen, Y. E., and Freeman, B. A. (2005) *Proc. Natl. Acad. Sci. U.S.A.* **102,** 2340–2345
21. Baker, P. R., Lin, Y., Schopfer, F. J., Woodcock, S. R., Groeger, A. L., Batthyany, C., Sweeney, S., Long, M. H., Iles, K. E., Baker, L. M., Branchaud, B. P., Chen, Y. E., and Freeman, B. A. (2005) *J. Biol. Chem.* **280,** 42464–42475
22. Itoh, T., Fairall, L., Amin, K., Inaba, Y., Szanto, A., Balint, B. L., Nagy, L., Yamamoto, K., and Schwabe, J. W. (2008) *Nat. Struct. Mol. Biol.* **15,** 924–931
23. Lehmann, J. M., Moore, L. B., Smith-Oliver, T. A., Wilkison, W. O., Willson, T. M., and Kliewer, S. A. (1995) *J. Biol. Chem.* **270,** 12953–12956

24. Young, P. W., Buckle, D. R., Cantello, B. C., Chapman, H., Clapham, J. C., Coyle, P. J., Haigh, D., Hindley, R. M., Holder, J. C., Kallender, H., Latter, A. J., Lawrie, K. W., Mossakowska, D., Murphy, G. J., Roxbee Cox, L., and Smith, S. A. (1998) *J. Pharmacol. Exp. Ther.* **284,** 751–759
25. Nissen, S. E., and Wolski, K. (2007) *N. Engl. J. Med.* **356,** 2457–2471
26. Nissen, S. E., Wolski, K., and Topol, E. J. (2005) *JAMA* **294,** 2581–2586
27. Woodcock, S. R., Marwitz, A. J., Bruno, P., and Branchaud, B. P. (2006) *Org. Lett.* **8,** 3931–3934
28. Baker, P. R., Schopfer, F. J., Sweeney, S., and Freeman, B. A. (2004) *Proc. Natl. Acad. Sci. U.S.A.* **101,** 11577–11582
29. Bouvier, G., Benoliel, A. M., Foa, C., and Bongrand, P. (1994) *J. Leukocyte Biol.* **55,** 729–734
30. Rudolph, V., Schopfer, F. J., Khoo, N. K., Rudolph, T. K., Cole, M. P., Woodcock, S. R., Bonacci, G., Groeger, A. L., Golin-Bisello, F., Chen, C. S., Baker, P. R., and Freeman, B. A. (2009) *J. Biol. Chem.* **284,** 1461–1473
31. Hu, X., Feng, Y., Shen, Y., Zhao, X. F., Yu, J. H., Yang, Y. S., and Leng, Y. (2006) *Acta Pharmacol. Sin.* **27,** 1346–1352
32. Li, Y., Zhang, J., Schopfer, F. J., Martynowski, D., Garcia-Barrio, M. T., Kovach, A., Suino-Powell, K., Baker, P. R., Freeman, B. A., Chen, Y. E., and Xu, H. E. (2008) *Nat. Struct. Mol. Biol.* **15,** 865–867
33. Shiraki, T., Kodama, T. S., Shiki, S., Nakagawa, T., and Jingami, H. (2006) *Biochem. J.* **393,** 749–755
34. Waku, T., Shiraki, T., Oyama, T., Fujimoto, Y., Maebara, K., Kamiya, N., Jingami, H., and Morikawa, K. (2009) *J. Mol. Biol.* **385,** 188–199
35. Li, Y., Wang, Z., Furukawa, N., Escaron, P., Weiszmann, J., Lee, G., Lindstrom, M., Liu, J., Liu, X., Xu, H., Plotnikova, O., Prasad, V., Walker, N., Learned, R. M., and Chen, J. L. (2008) *J. Biol. Chem.* **283,** 9168–9176
36. Nettles, K. W. (2008) *Nat. Struct. Mol. Biol.* **15,** 893–895
37. Zhang, F., Lavan, B. E., and Gregoire, F. M. (2007) *PPAR Res.* **2007,** 32696
38. Wigren, J., Surapureddi, S., Olsson, A. G., Glass, C. K., Hammarström, S., and Söderström, M. (2003) *J. Endocrinol.* **177,** 207–214
39. Feige, J. N., and Auwerx, J. (2007) *Trends Cell Biol.* **17,** 292–301
40. Guan, Y., Hao, C., Cha, D. R., Rao, R., Lu, W., Kohan, D. E., Magnuson, M. A., Redha, R., Zhang, Y., and Breyer, M. D. (2005) *Nat. Med.* **11,** 861–866
41. Khanderia, U., Pop-Busui, R., and Eagle, K. A. (2008) *Ann. Pharmacother.* **42,** 1466–1474
42. Carmona, M. C., Louche, K., Lefebvre, B., Pilon, A., Hennuyer, N., Audinot-Bouchez, V., Fievet, C., Torpier, G., Formstecher, P., Renard, P., Lefebvre, P., Dacquet, C., Staels, B., Casteilla, L., and Pénicaud, L. (2007) *Diabetes* **56,** 2797–2808